Electronic Supplementary Material (ESI) for RSC Advances.

Revealing biomedically relevant cell and lectin type-dependent structure-activity profiles for glycoclusters by using tissue sections as assay platform

Herbert Kaltner,[a] Joachim C. Manning,[a] Gabriel García Caballero,[a] Claudia Di Salvo,[b] Adele Gabba,[b] Laura Romero,[b] Clemens Knospe,[c] Dan Wu,[d] Harrison Daly,[d] Donal F. O'Shea,[d] Hans-Joachim Gabius[a] and Paul V. Murphy[*b]

[a]Institute of Physiological Chemistry, Faculty of Veterinary Medicine, Ludwig-Maximilians-University Munich, Veterinärstr. 13, 80539 Munich, Germany

[b]School of Chemistry, National University of Ireland Galway, University Road, Galway, Ireland

[c]Institute of Anatomy, Histology and Embryology, Faculty of Veterinary Medicine, Ludwig-Maximilians-University Munich, Veterinärstr. 13, 80539 Munich, Germany

[d]Department of Chemistry, Royal College of Surgeons of Ireland (RCSI), 123 St. Stephen's Green, Dublin 2, Ireland

[*]to whom correspondence should be addressed

e-mail: paul.v.murphy@nuigalway.ie

Supplementary Information Section

Content:

^{1}H NMR (500 MHz, $CDCl_3$) 11

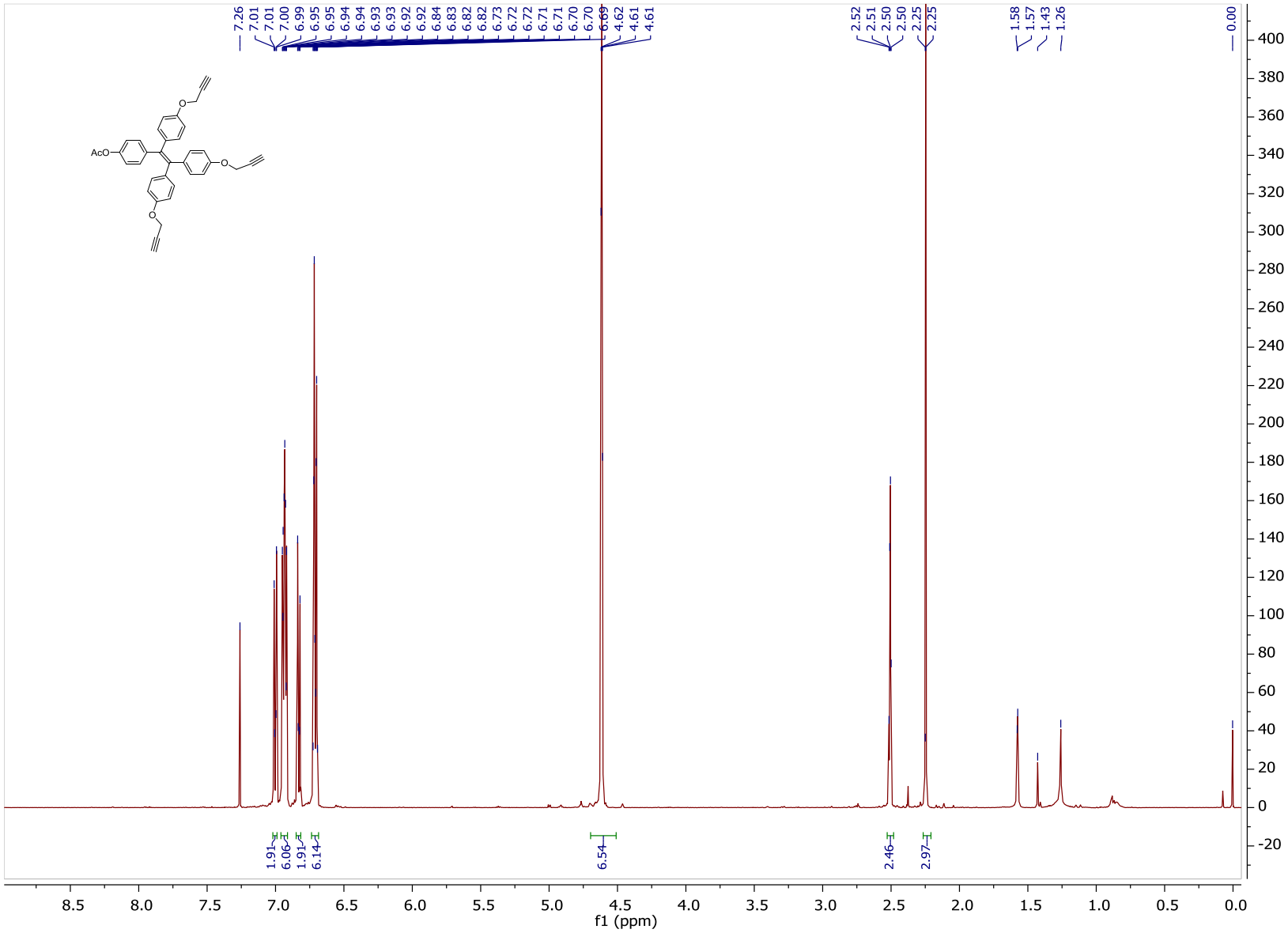

^{13}C NMR (126 MHz, $CDCl_3$) 11

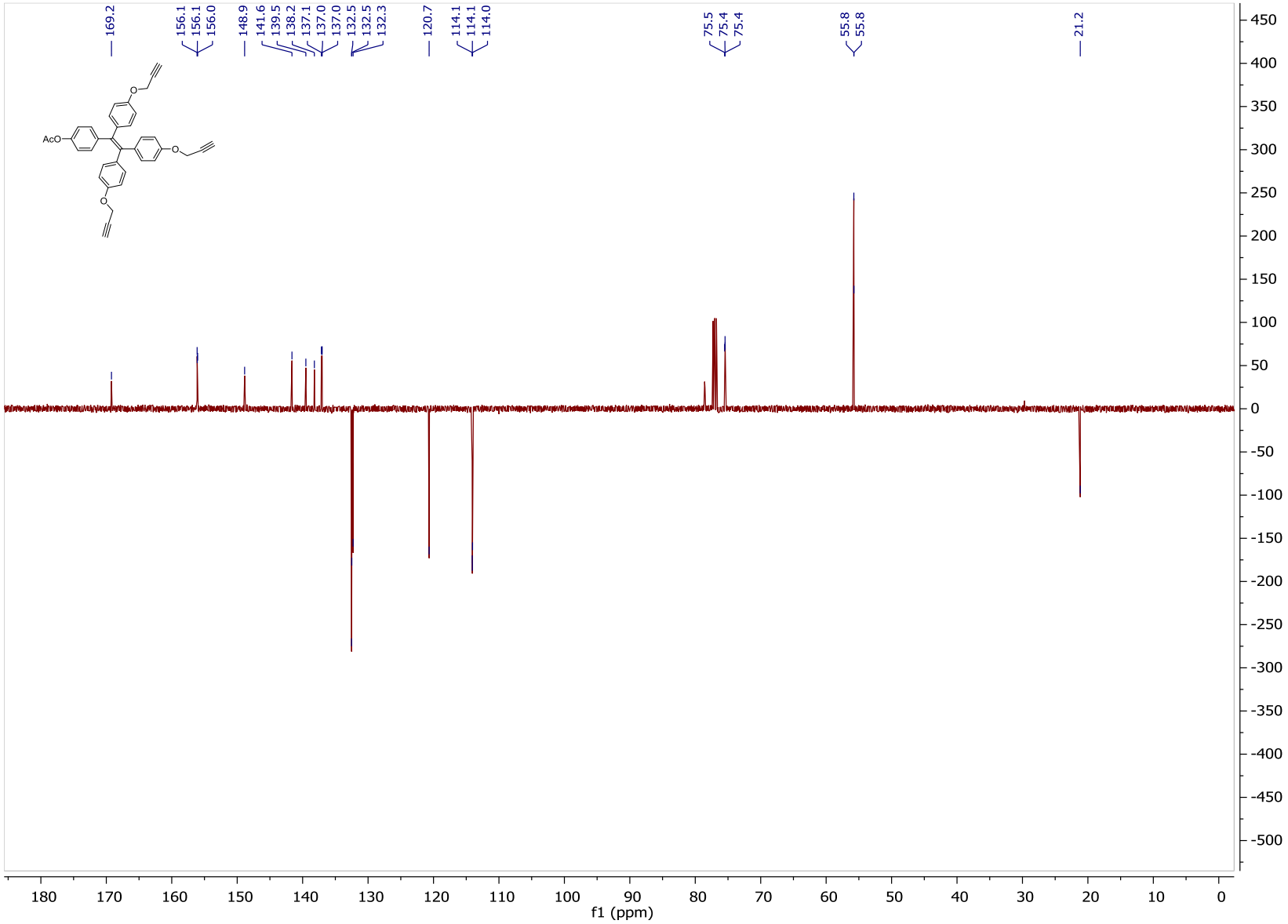

^{1}H NMR (500 MHz, DMSO-d_6) 3

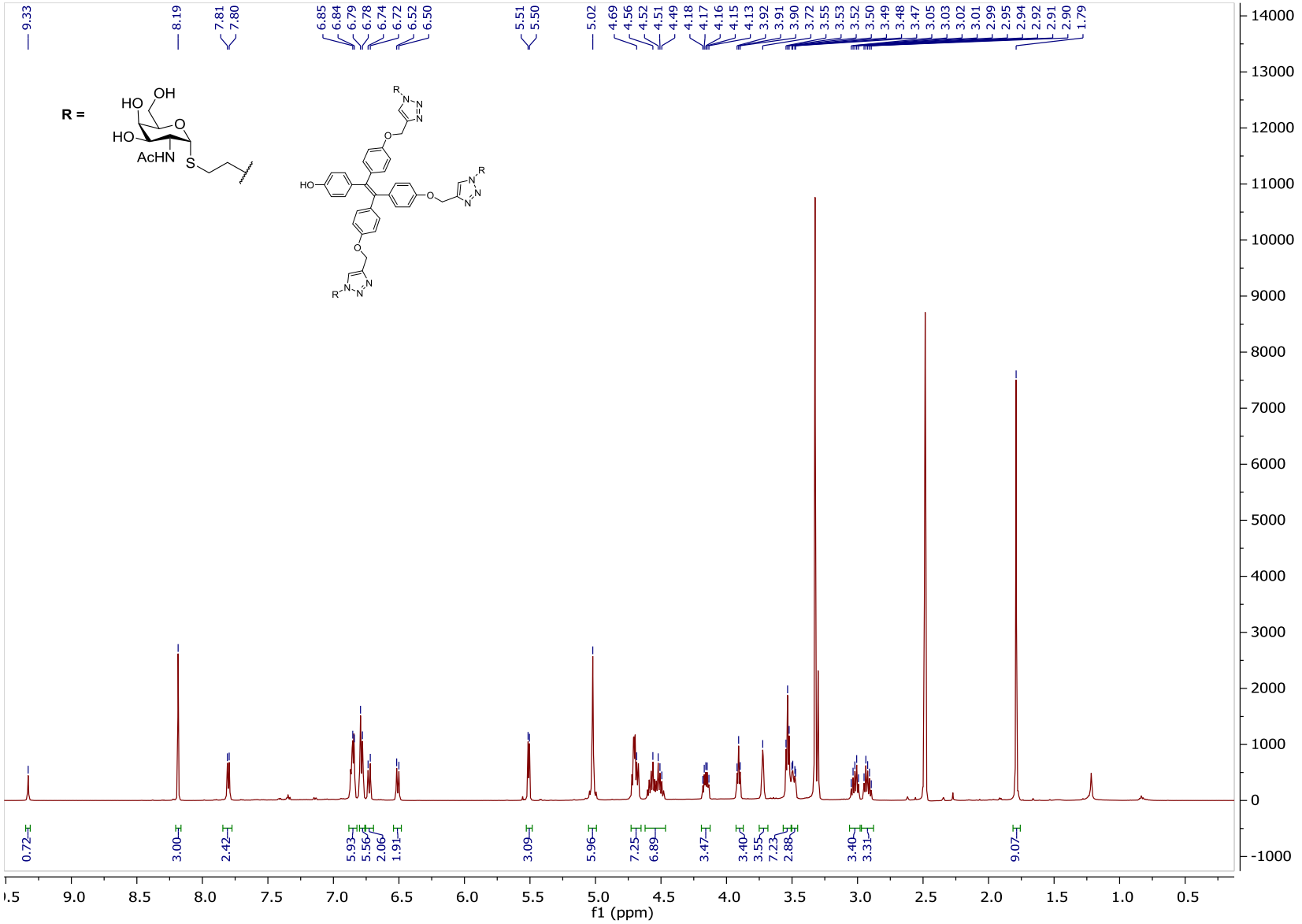

^{13}C-NMR (126 MHz, DMSO-d_6) 3

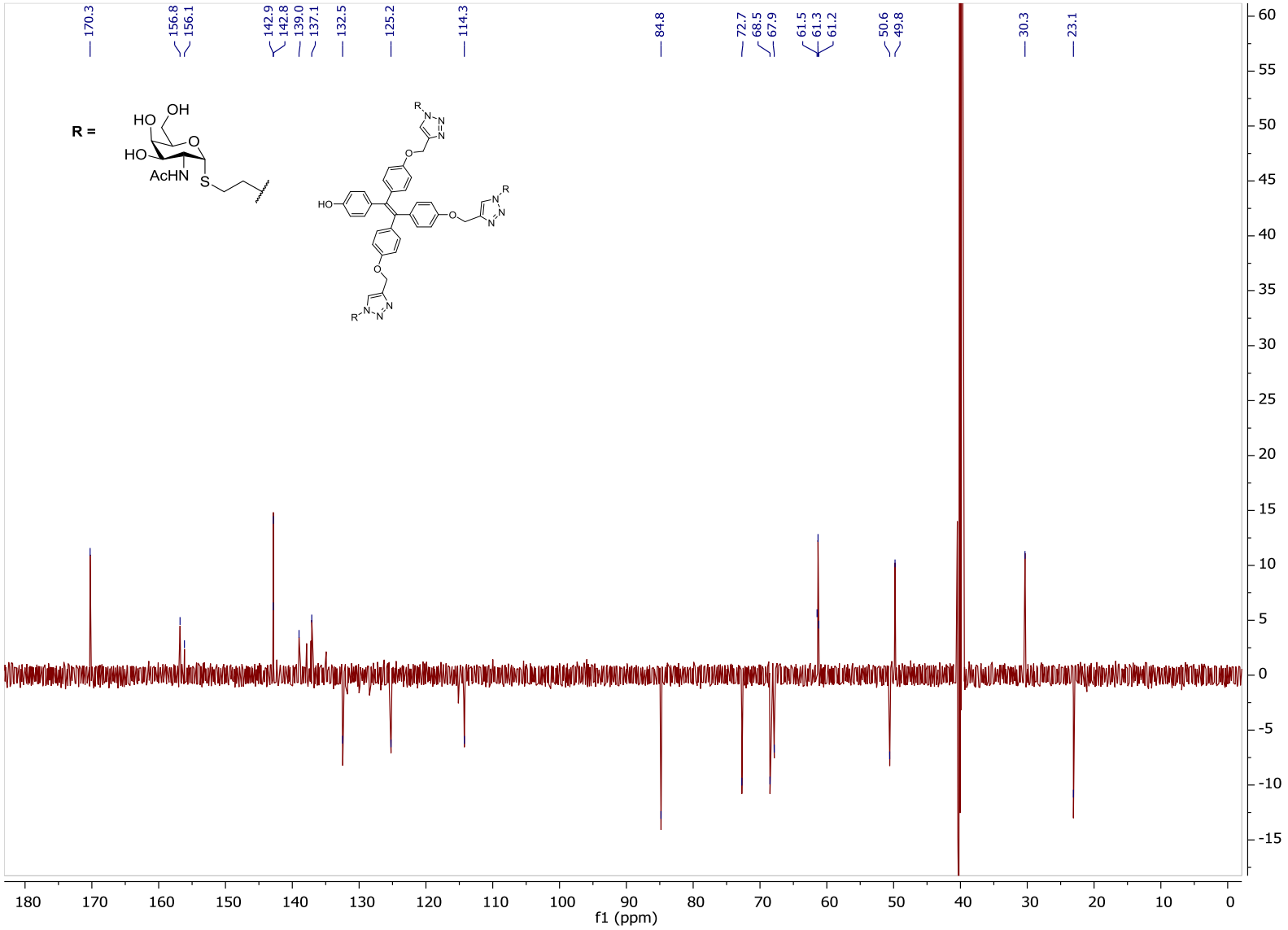

^{1}H NMR (500 MHz, $CDCl_3$) 14

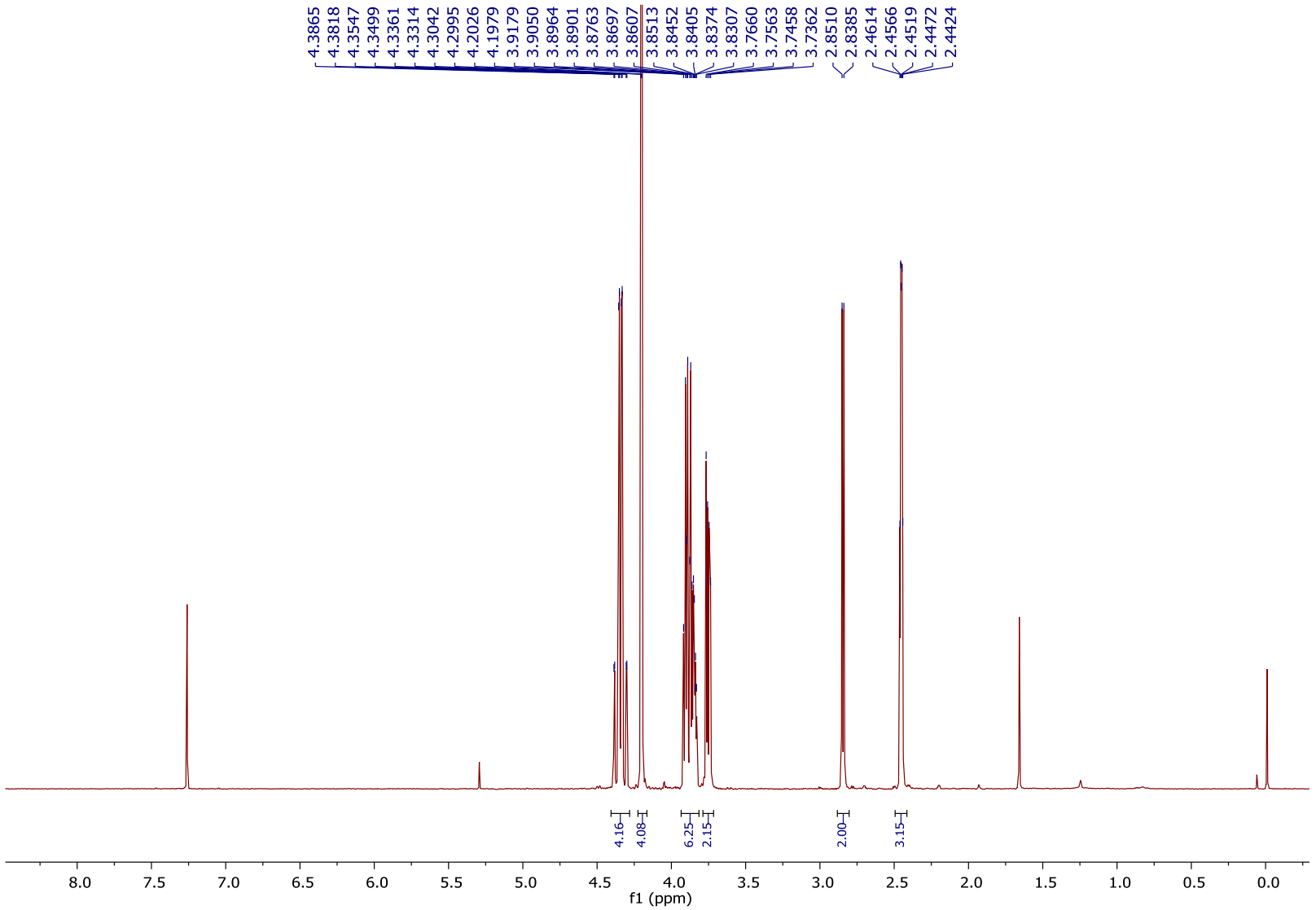

^{13}C NMR (126 MHz, $CDCl_3$) 14

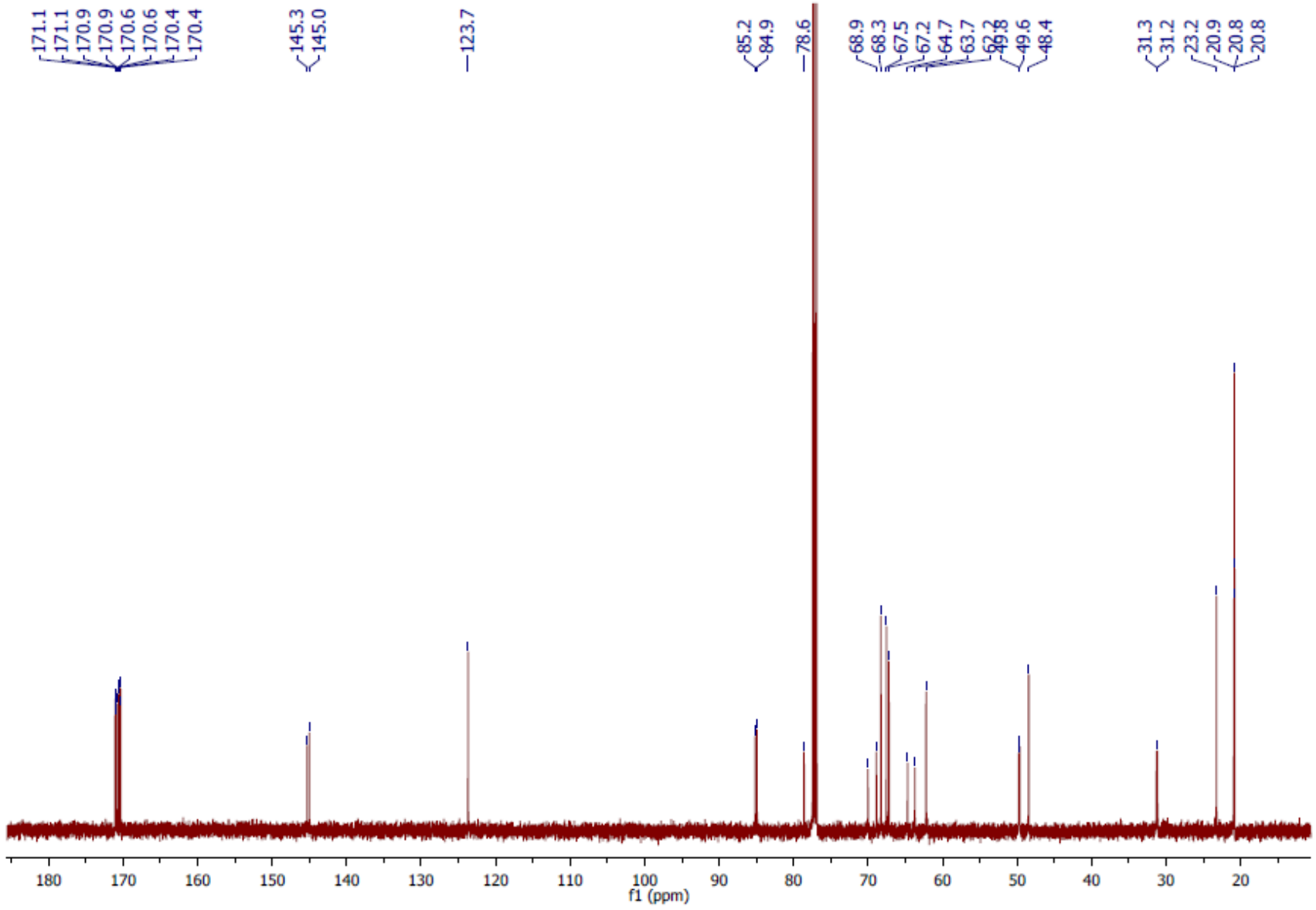

^{1}H NMR (500 MHz, DMSO-d_6) 4

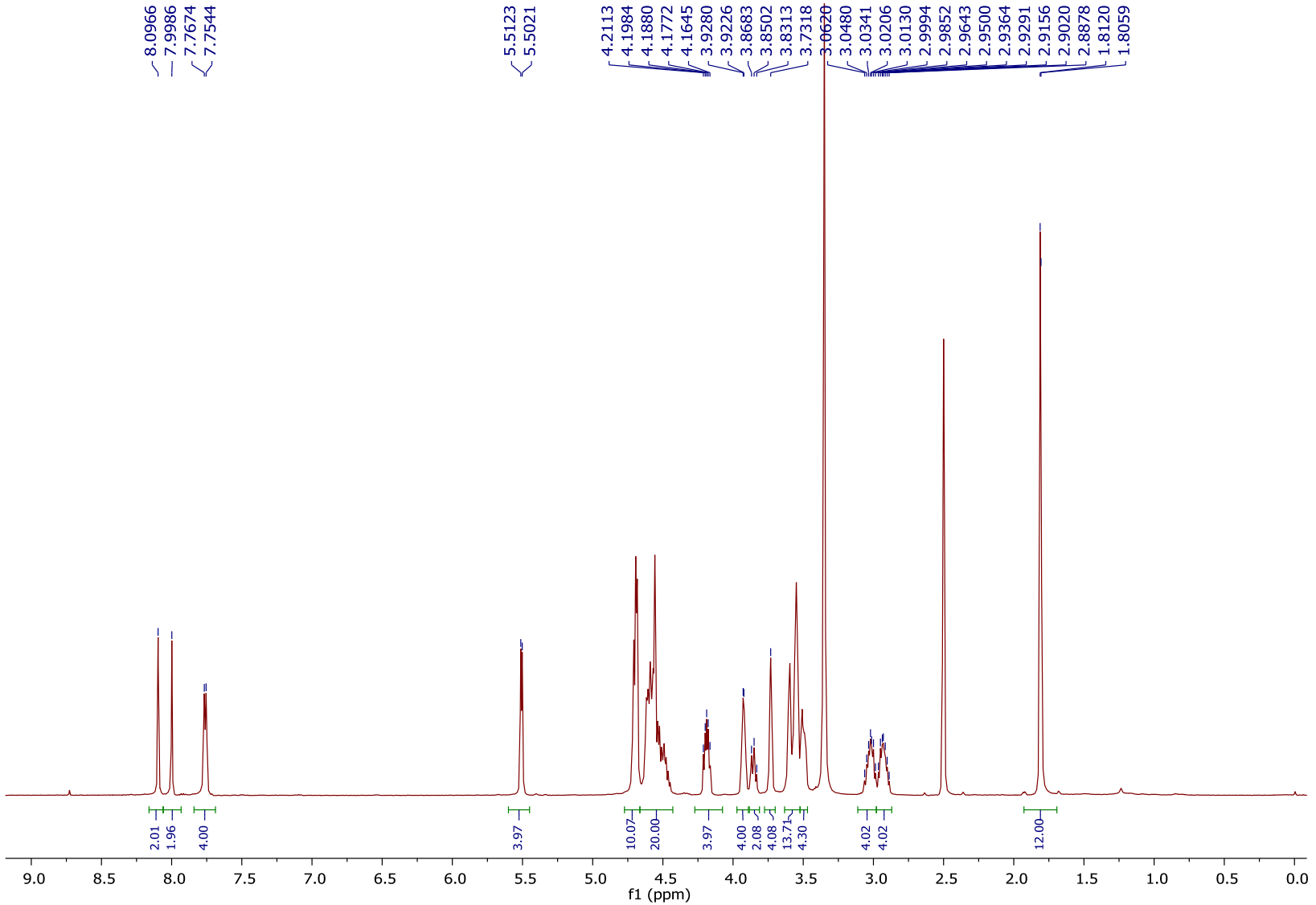

^{13}C NMR (126 MHz, DMSO-d_6) 4

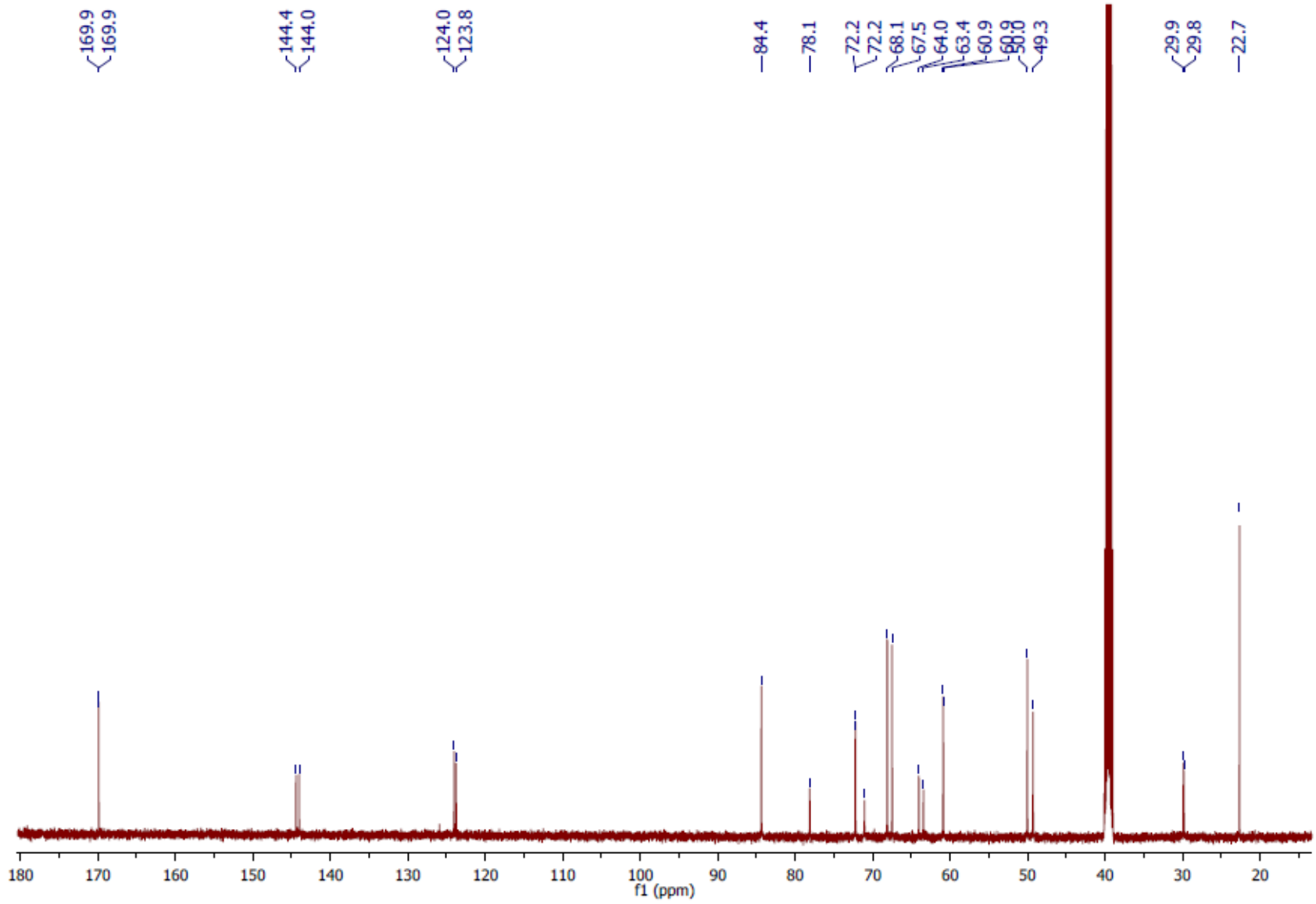

^{1}H NMR (400 MHz, DMSO-d_6) 16

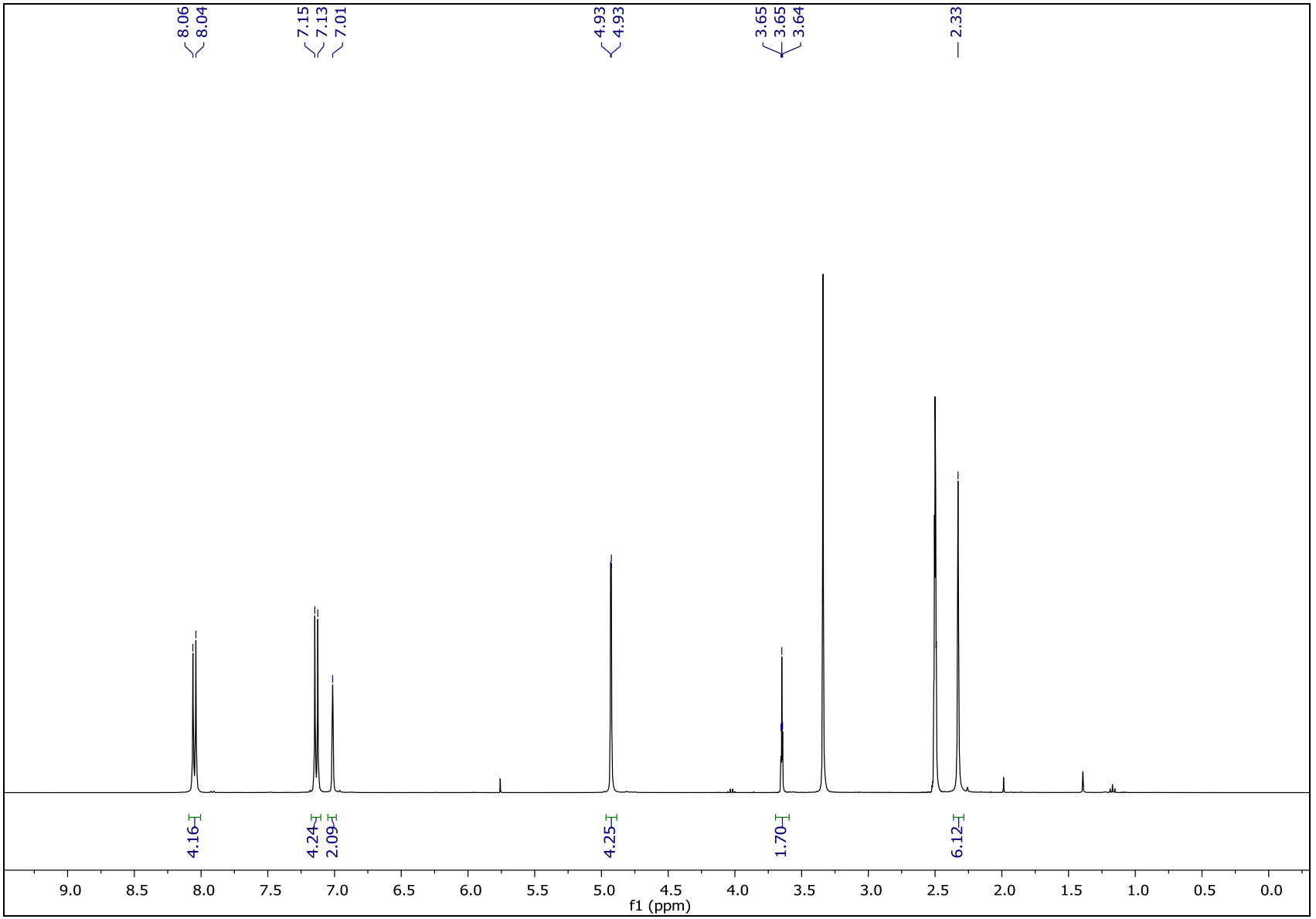

^{13}C NMR (100 MHz, DMSO-d_6) 16

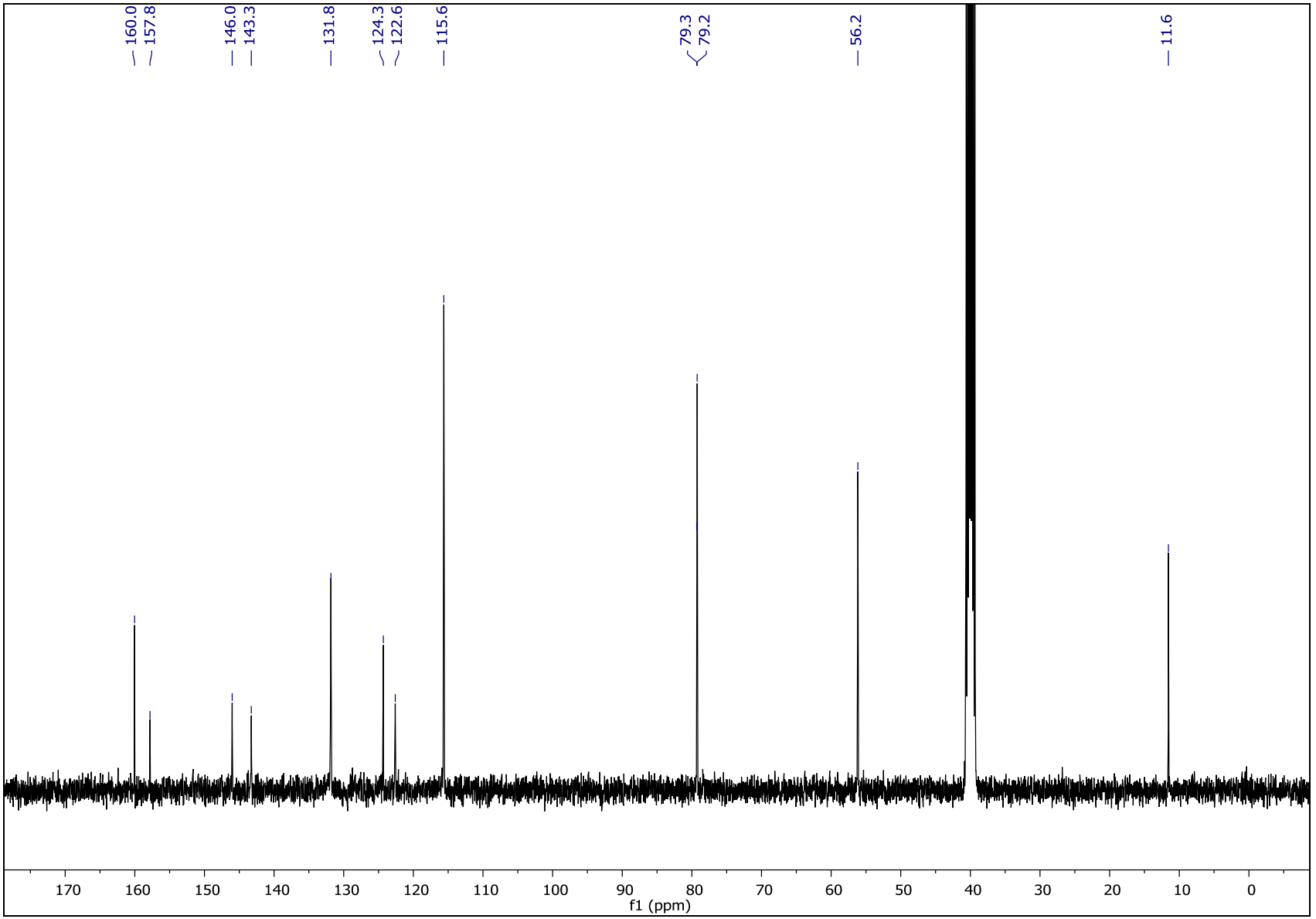

^{1}H NMR (500 MHz, DMSO-d_6) 6

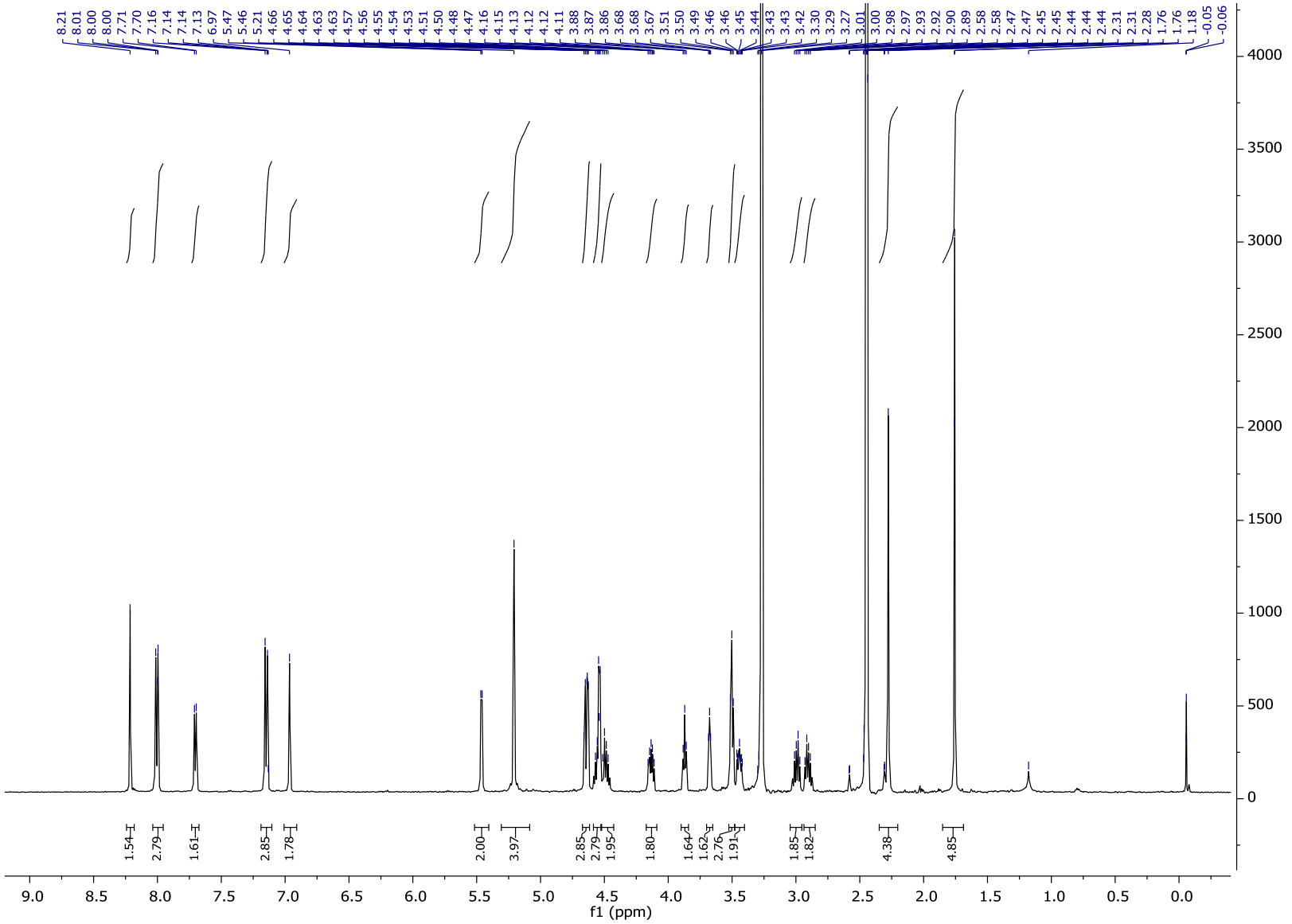

^{13}C NMR (126 MHz, DMSO-d_6) 6

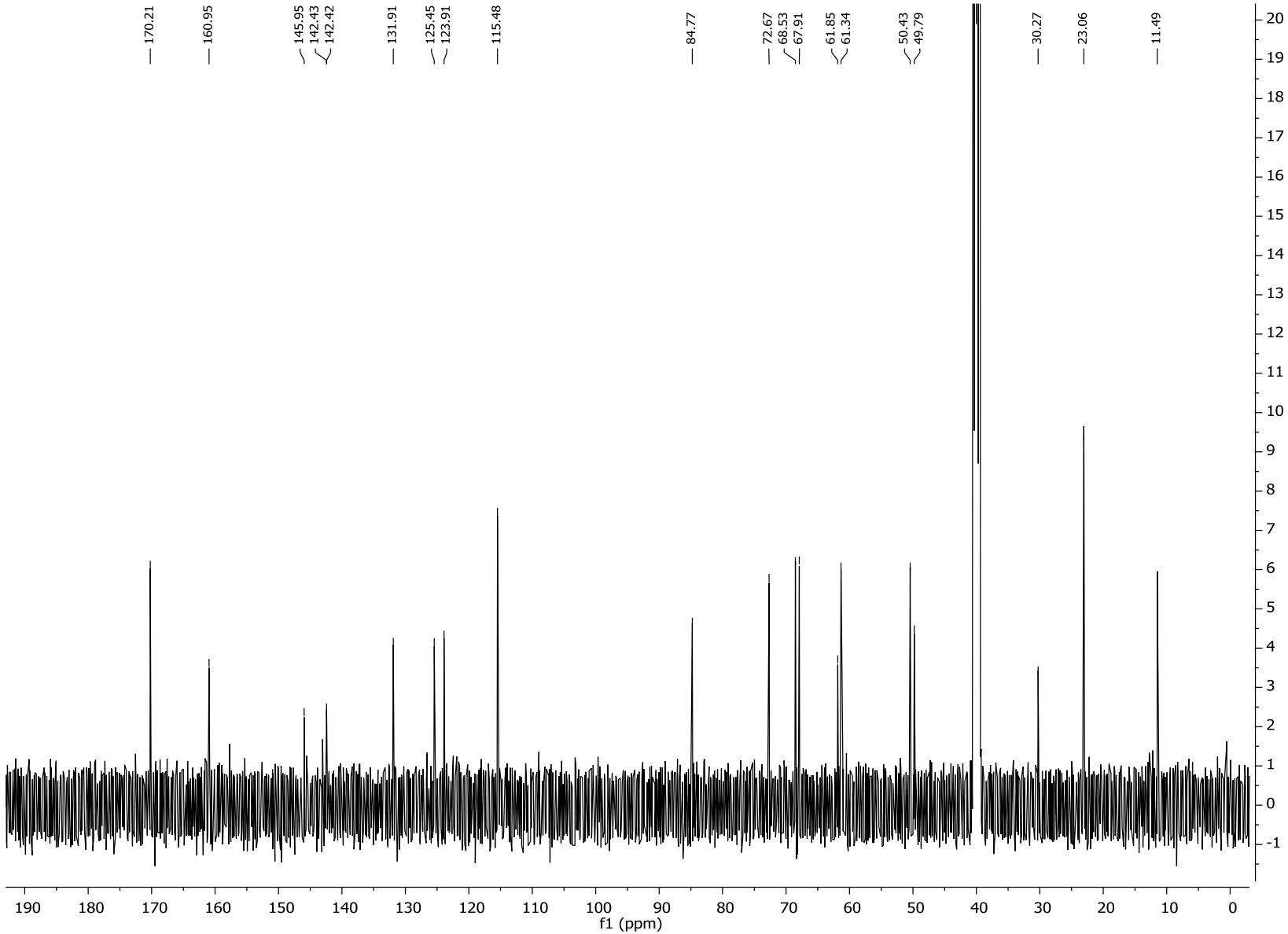

^{1}H NMR (500 MHz, methanol-d_4) 7

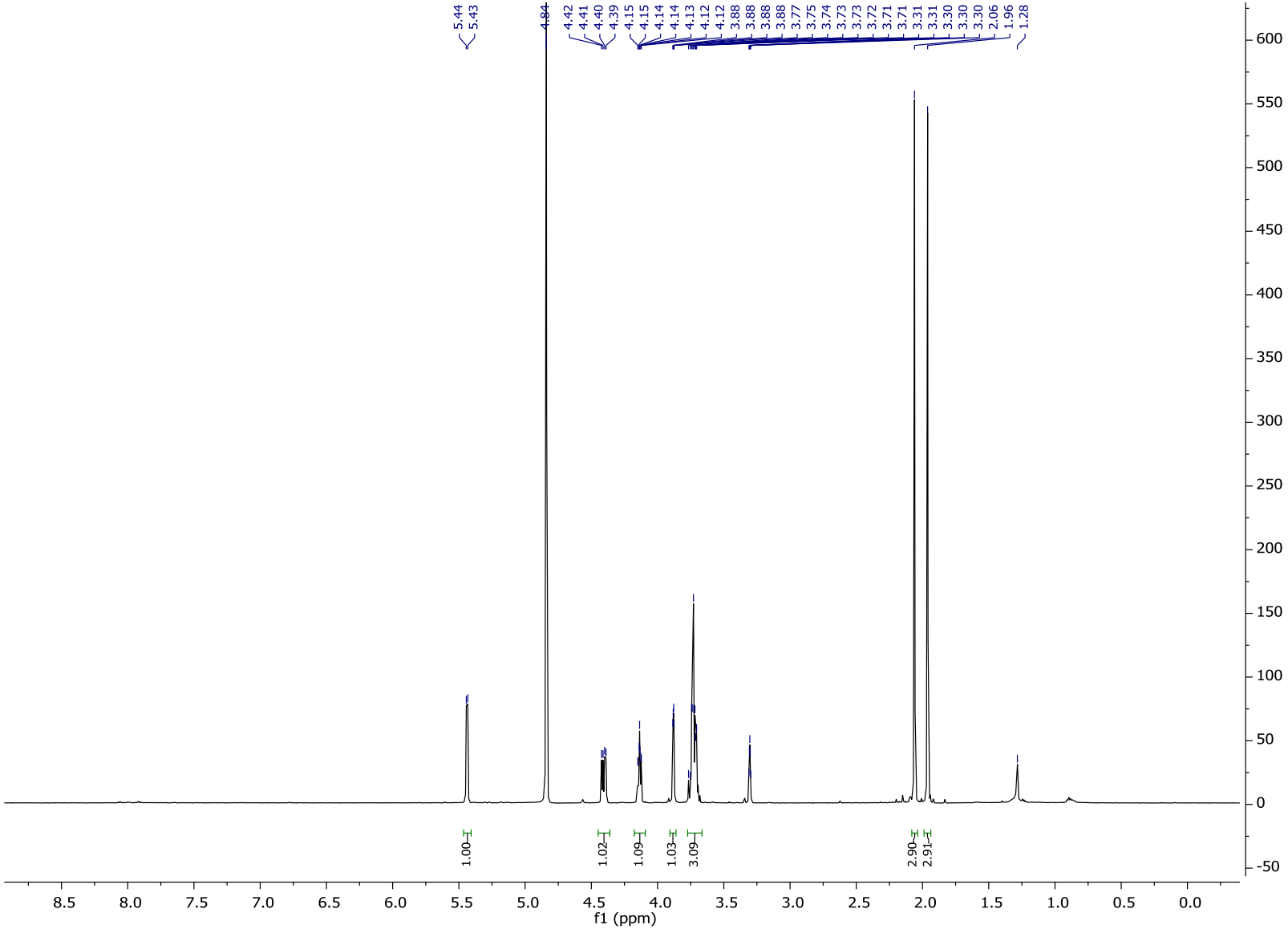

^{13}C NMR (126 MHz, methanol-d_4) 7

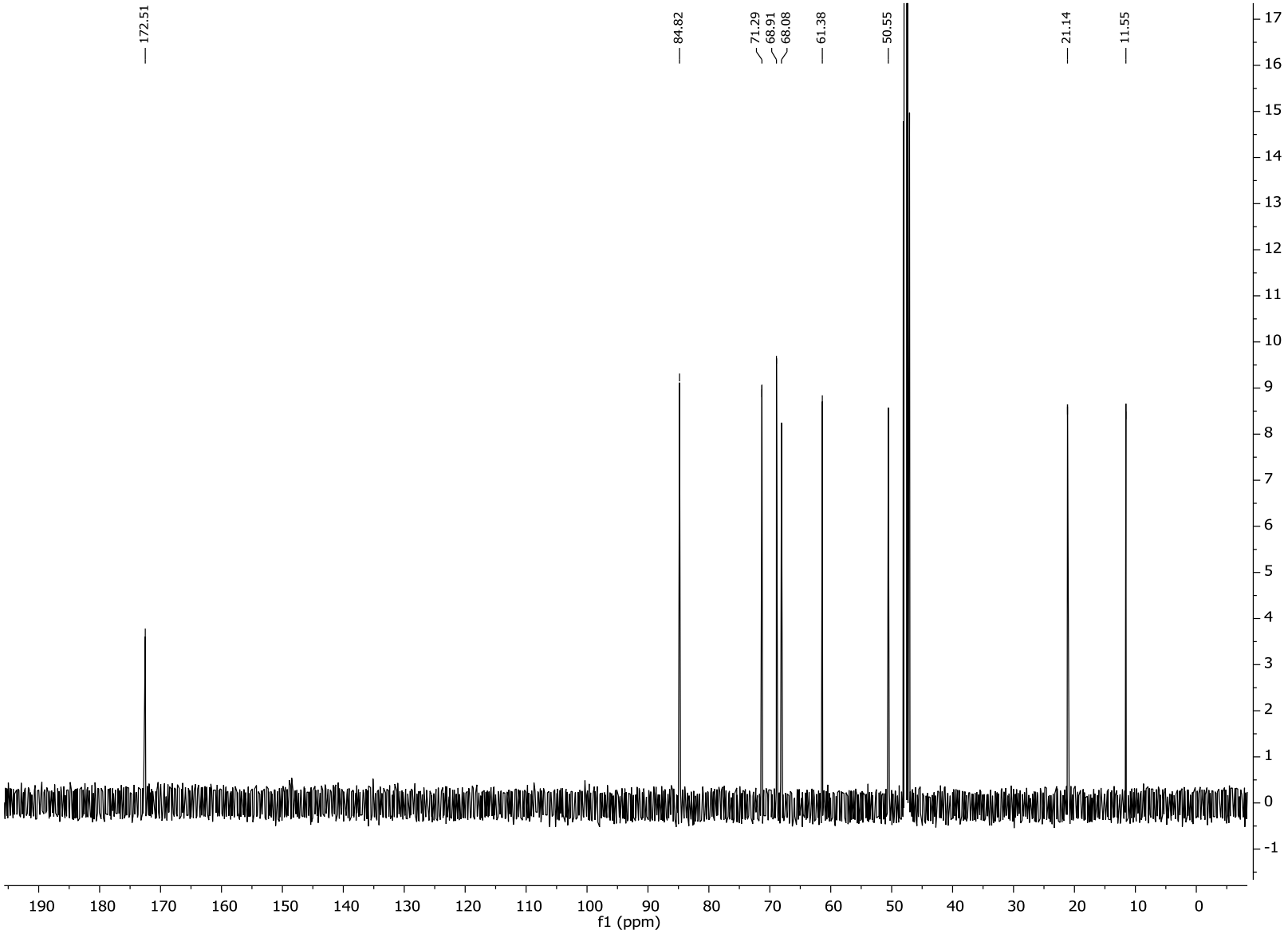

^{1}H NMR (500 MHz, methanol-d_4) 19

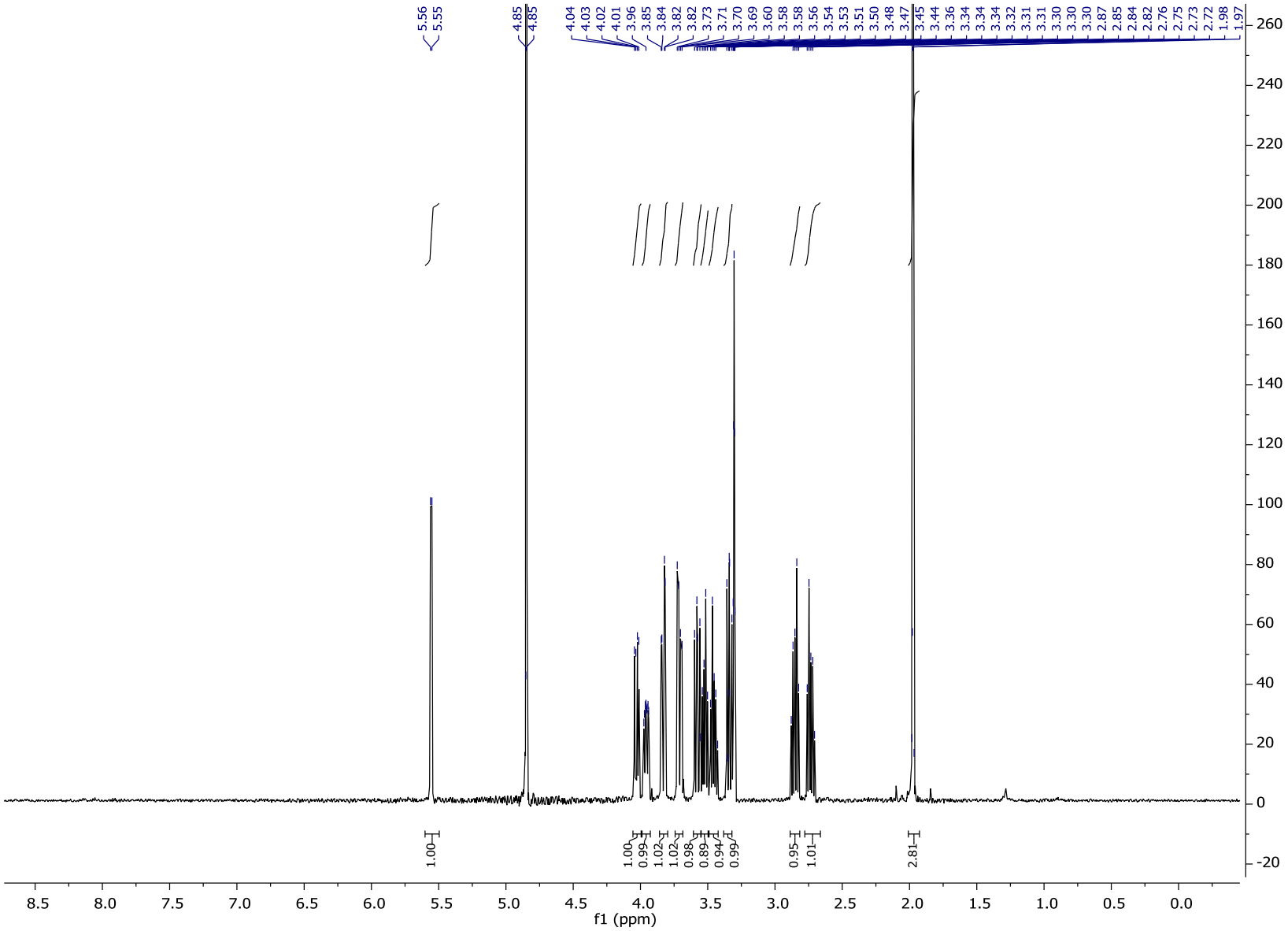

^{13}C NMR (126 MHz, methanol-d_4) 19

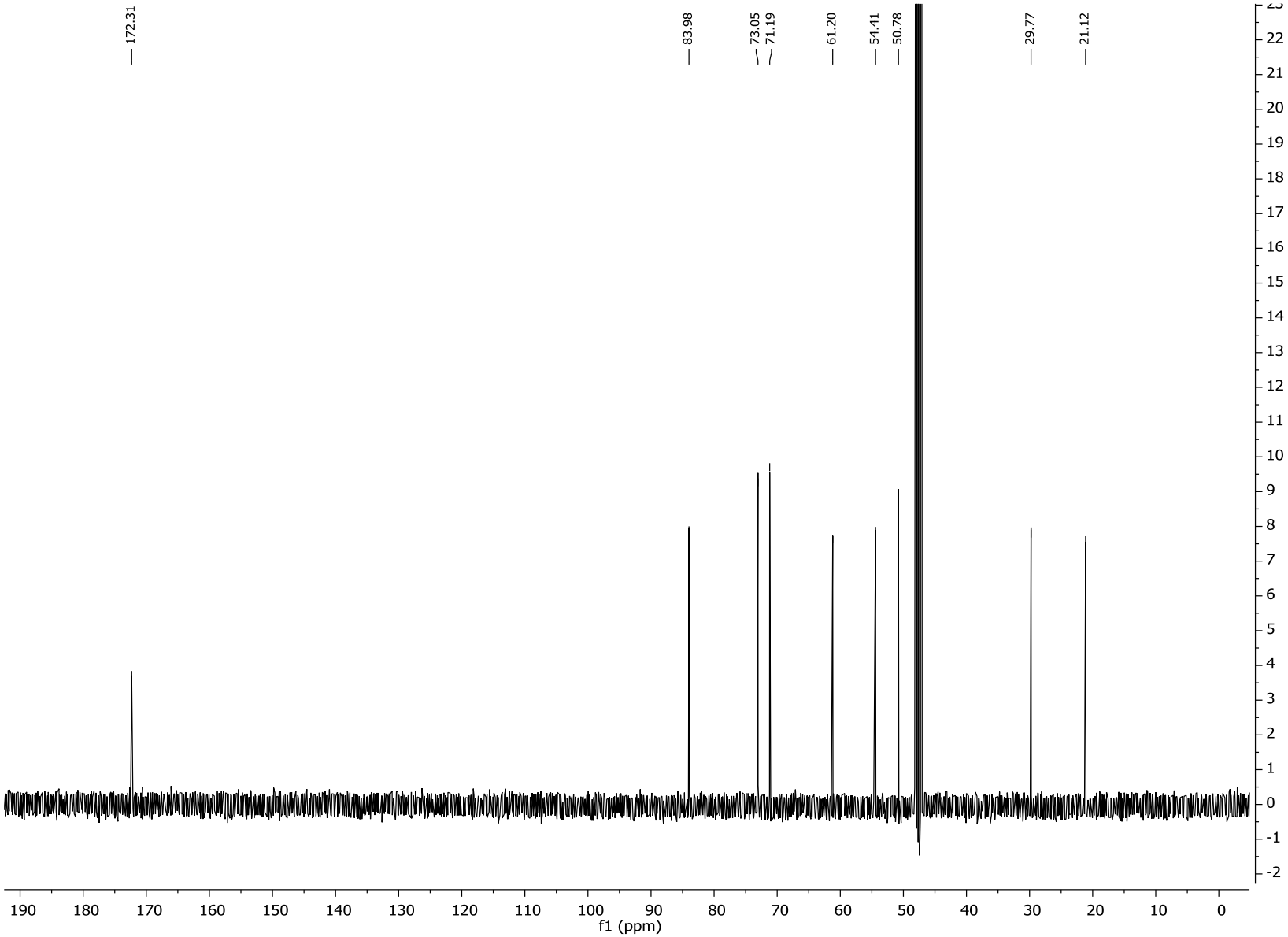

^{1}H NMR (500 MHz, methanol-d_4) 8

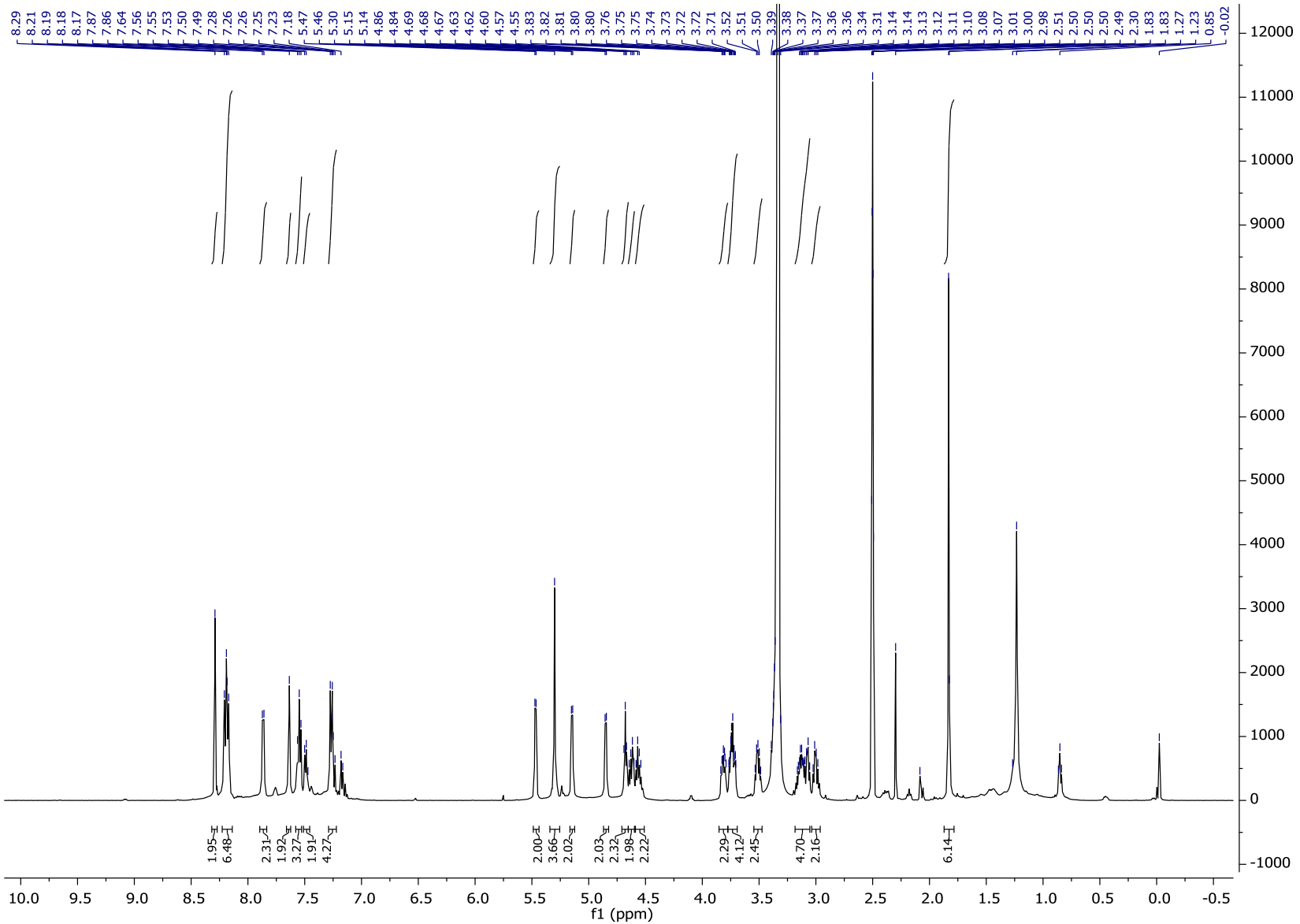

^{13}C NMR (126 MHz, methanol-d_4) 8

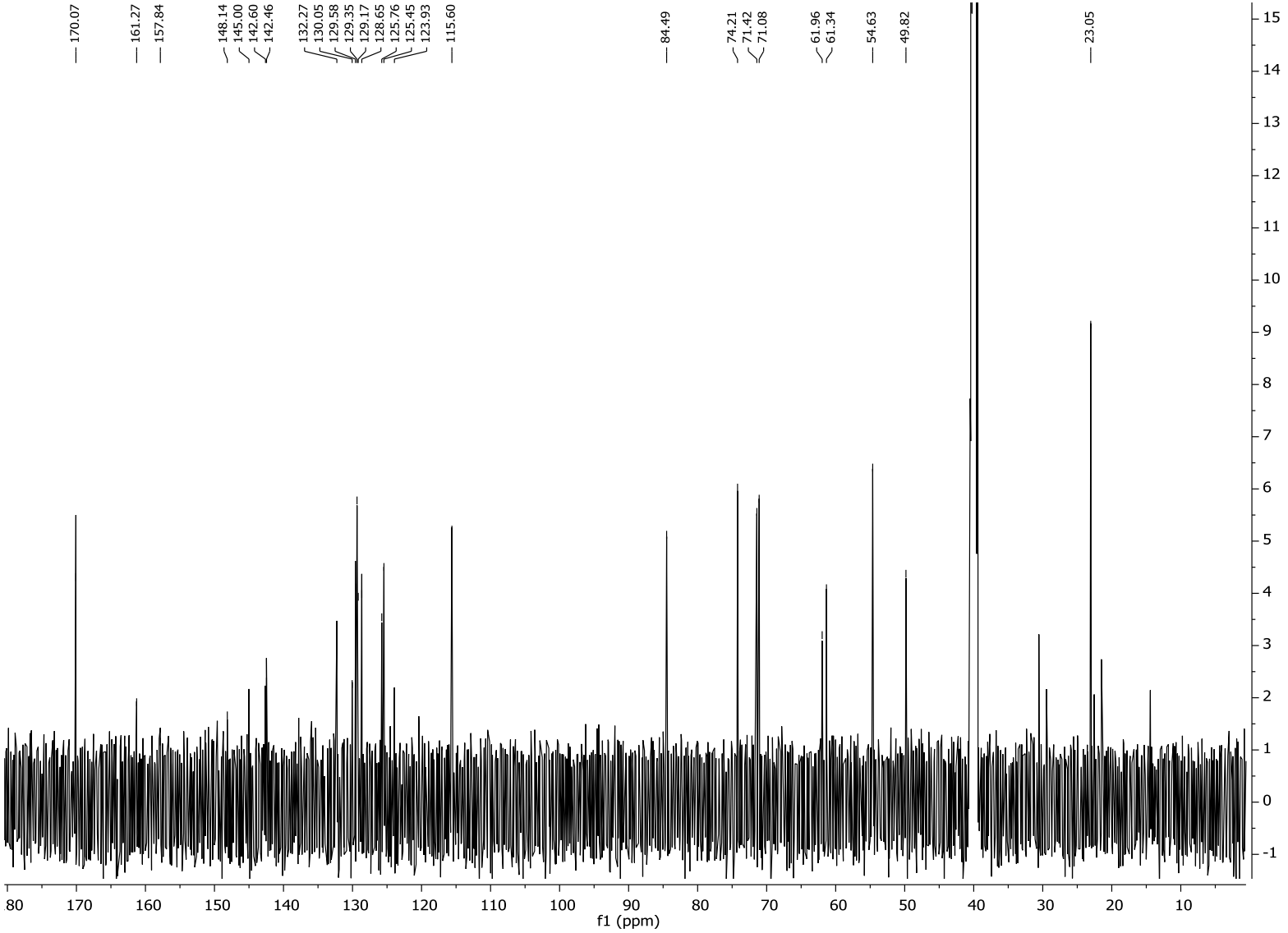

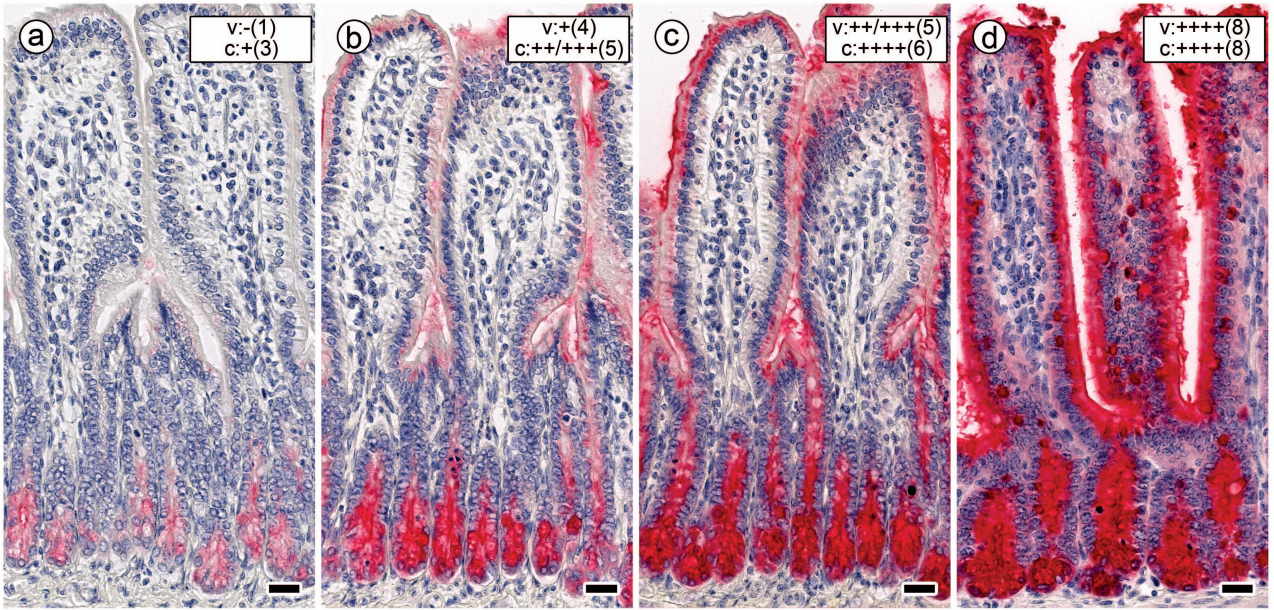

Fig. S1 Illustration of dependence of level of positivity on lectin (biotinylated SBA) concentration (tested at four concentrations) in longitudinal sections of fixed murine jejunum. The second-step reagent avidin - alkaline phosphatase conjugate together with the substrate Vector® Red was used for signal generation. Incubation with the lowest lectin concentration (0.5 µg/ml) resulted in weak staining intensity and low percentage of positive cells, positivity restricted to intestinal crypts (**a**). Signal intensity and percentage of positive cells increased at this site when stepwisely increasing the SBA concentration (**b** 1 µg/ml; **c** 2 µg/ml; **d** 3 µg/ml). Staining appeared in surface enterocytes of intestinal villi and goblet cells. Category of semiquantitative grading of the staining intensity and of percentage of positive cells is given in the top-right area of each microphotograph (categories for staining intensity and percentage of cells are given in detail in the legend for Fig. 6). Scale bars are 20 µm.

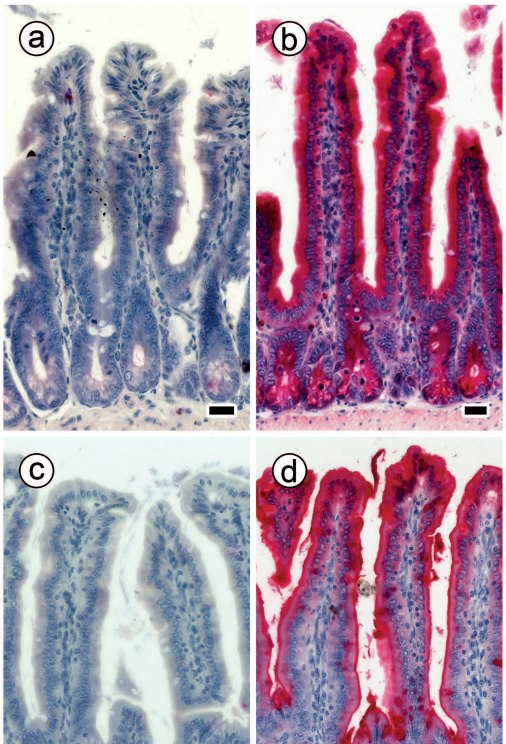

Fig. S2 Illustration of specificity controls when applying biotinylated MGL (CRD + stalk) and SBA to longitudinal sections of fixed murine jejunum in the presence of cognate GalNAc or non-cognate sugar GlcNAc. Intestinal villi and crypts were mostly negative after processing with biotinylated MGL (CRD + stalk) in the presence of 0.5 mM GalNAc in compound **6** (**a**), whereas 0.5 mM GlcNAc in compound **8** led to no reduction in signal intensity and percentage of positive cells (**b**). Complete inhibition of SBA binding with 0.2 mM GalNAc in compound **5** (**c**) versus the 100% level of staining when using the same concentration of GlcNAc in compound **9** (**d**). Scale bars are 20 µm.

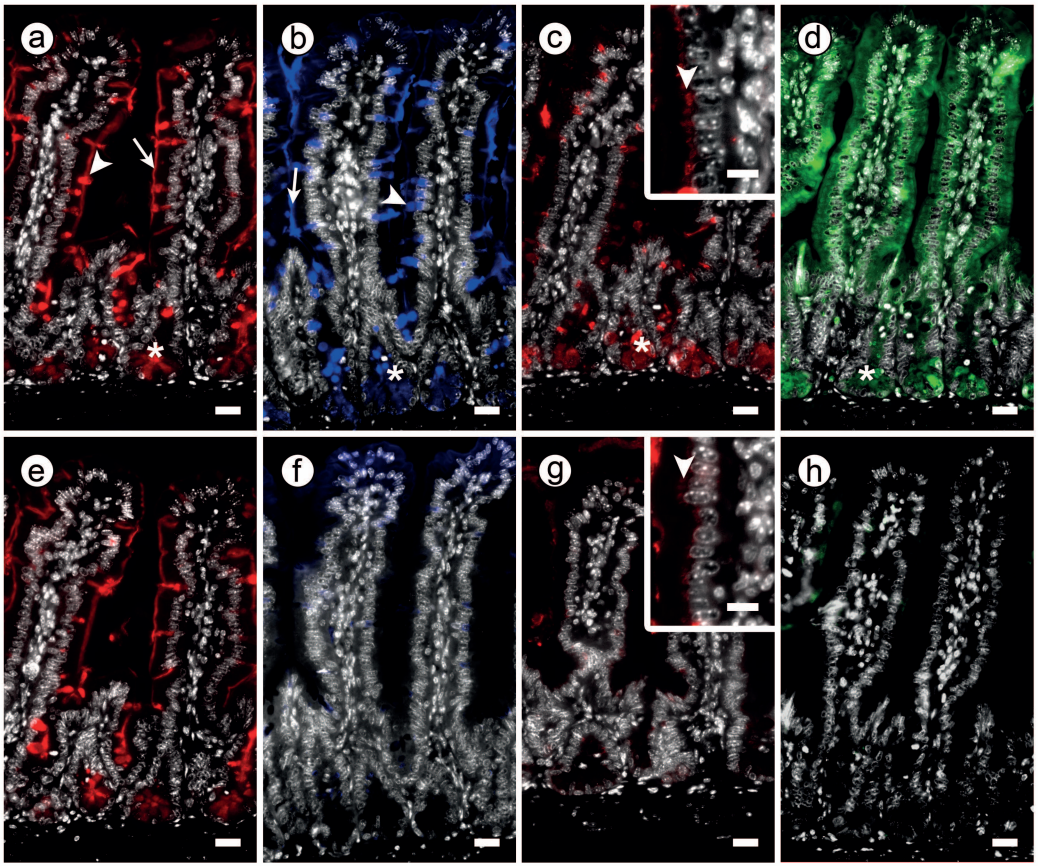

Fig. S3 Fluorescence staining profiles by DBA, SBA, HPA and MGL (CRD + stalk) in longitudinal sections of fixed murine jejunum in the absence or in the presence of cognate sugar (GalNAc in compound **5**). Sites of binding of biotinylated DBA and HPA were visualised with the second-step reagent Alexa Fluor®-647-conjugated streptavidin (5 µg/ml) (colour assignment in red), whereas SBA (conjugate with Alexa Fluor® 555; colour assignment in blue) and MGL (conjugate with FITC; green colour) were directly labelled. (**a**, **b**) DBA and SBA intensely stained the brush border of surface enterocytes in intestinal villi (arrows), crypt-associated cells (asterisks) and goblet cells (arrowheads). (**c**) HPA-dependent supranuclear staining of surface enterocytes from intestinal villi (inset: enlarged view of this region with arrowhead marking supranuclear staining) and in deep parts of crypts (asterisk). (**d**) MGL binding was seen in the cytoplasm of surface enterocytes and in the deep parts of crypts (asterisk). Co-incubation of lectin with 0.1 mM GalNAc (compound **5**) had no effect on DBA binding (**e**) but led to complete inhibition of SBA (**f**)- and MGL (**h**) -dependent staining, whereas weak HPA-dependent staining intensity was maintained supranuclearly (**g**; inset: enlarged view of this region with an arrowhead marking supranuclear staining). Staining of nuclei was performed with DAPI (0.5 µg/ml; colour assignment to white). Concentration of biotinylated DBA and HPA was 1 µg/ml, that of Alexa Fluor®-555-labelled SBA 2 µg/ml and FITC-labelled MGL 16 µg/ml. Scale bars are 20 µm.

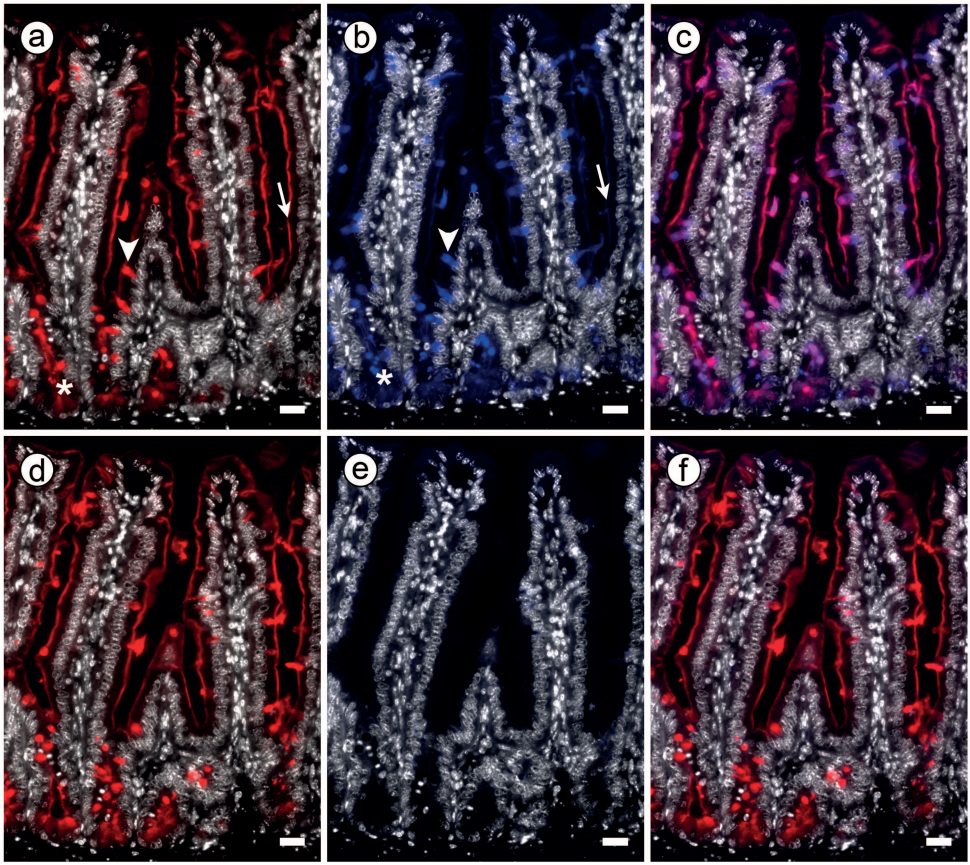

Fig. S4 Two-colour fluorescence staining patterns by a mixture of labelled DBA and SBA in longitudinal sections of fixed murine jejunum in the absence or in the presence of cognate sugar (GalNAc) in compound **5**. Accessible binding sites for the two lectins were visualised by applying biotinylated DBA and then Alexa Fluor®-647-labelled streptavidin (5 µg/ml; colour assignment to red) and Alexa Fluor®-555-labelled SBA (colour assignment to blue). DAPI (0.5 µg/ml) was used for staining of nuclei (colour assignment to white). (**a**-**c**) Binding of DBA (**a**) and SBA (**b**) in brush border (arrows), goblet cells (arrowheads) and crypt-associated cells (asterisks; please see also Fig. S3). Colour change to magenta was seen in regions of overlap, that is in parts of brush border and in goblet cells (**c**). (**d**-**f**) DBA-dependent binding was not impaired by the presence of 0.1 mM GalNAc (compound **5**) (**d**), whereas SBA-dependent binding was completely inhibited (**e**) so that (photo)merging led to exclusive visualisation of the DBA staining (**f**). Concentration of biotinylated DBA was 1 µg/ml, that of Alexa Fluor®-555-labelled SBA was 2 µg/ml. Scale bars are 20 µm.

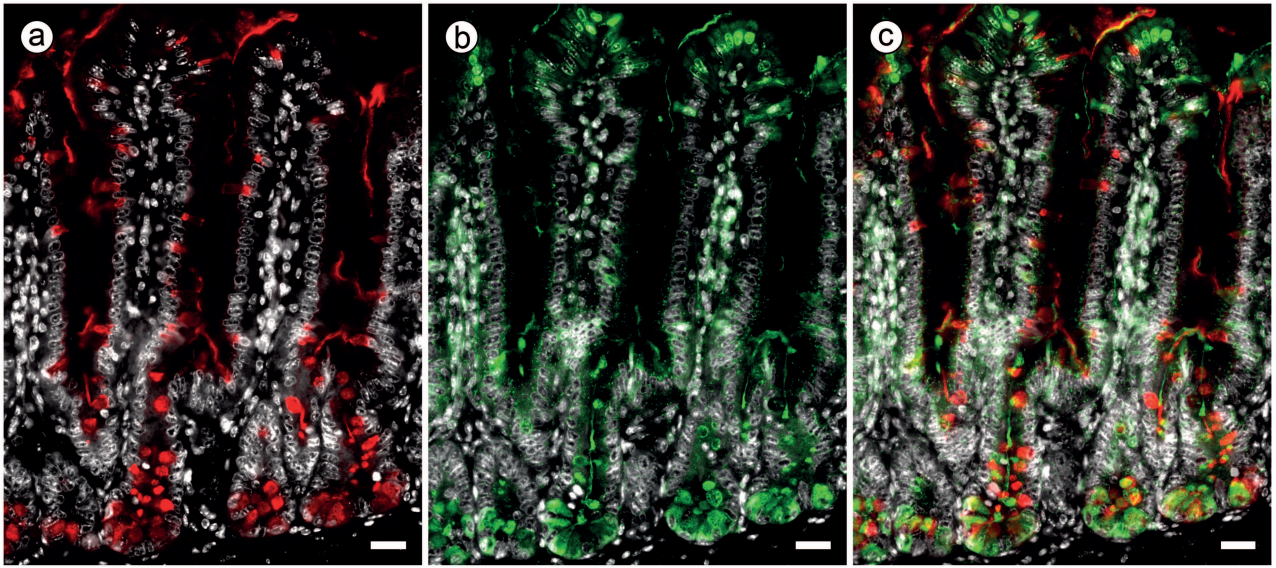

Fig. S5 Illustration of fluorescent staining using biotinylated HPA in two consecutive longitudinal sections of fixed murine jejunum. Binding sites were visualised using Alexa Fluor®-647-conjugated streptavidin (5 µg/ml) (colour assignment in red, **a**) or FITC-conjugated avidin (10 µl/ml) (colour assignment in green, **b**). Nuclei were stained by DAPI (0.5 µg/ml; colour assignment in white). The resulting (photo)merging, shown in **c**, illustrates occurrence of spatial changes in signal distribution, with limited areas of overlay (yellow) mainly seen in crypts. Concentration of biotinylated HPA was 2 µg/ml. Scale bars are 20 µm.